Comparative study of betatron radiation from different injection mechanisms in a gas jet

Contact: savio.rozario11@imperial.ac.uk

S. V. Rozario, E. Gerstmayer, J. M. Cole, N. C. Lopes, K. Poder, J. C. Wood, S. P. D. Mangles, Z. Najmudin
The John Adams Institute for Accelerator Science
Blackett Laboratory,
Imperial College London,
SW7 2AZ, UK

D. R. Symes, N. Booth, N. Bourgeois, O. Chekhlov, S. J. Hawkes, C. J. Hooker, P. P. Rajeev
Central Laser Facility,
STFC Rutherford Appleton Laboratory,
Didcot, OX11 0QX, UK

Introduction

High power laser systems have enabled the development of the compact particle accelerators, using plasma, as the accelerating medium. As plasmas are already 'broken down', they can sustain orders of magnitude greater accelerating fields than conventional particle accelerators. Electron beams with beam energies in the GeV range are routinely generated using the Gemini laser facility using the technique known as Laser Wakefield acceleration (LWFA) [1–4]. A useful by-product of these accelerators is the generation of hard x-ray radiation, called betatron radiation [5, 6], capable of imaging various objects [7]. This radiation is generated by electrons oscillating in the focusing field present in this accelerator. We present data comparing the properties of betatron radiation with three different types of medium, helium, helium +1% nitrogen and methane and explore the various merits of each medium.

Injection mechanisms

The way in which particles are injected into an accelerator has a significant impact on the final properties of the electron beam and betatron radiation. Various mechanisms have been proposed. In this report, we explore self-injection, ionisation injection and cluster injection. Self-injection [8] occurs when the plasma wave undergoes wave-breaking. Some of the electrons, which form part of the wave, break free and are injected into the plasma wave. This phenomenon occurs in non-linear plasma waves when the amplitude of the wave is large enough for wave-breaking to occur. Ionisation injection [9–11] consists of doping the medium with a high Z gas. The binding energy of these electrons is high enough that they are ionised near the peak of the laser pulse. This delayed generation of electrons allows them to experience a reduced ponderomotive push by the laser pulse and be subsequently trapped by the plasma wave. A cluster is a collection of atoms 100s-100,000s atoms/ molecules large. They can be created in supersonic gas jets where gases undergo adiabatic cooling and condense to create solid density collection of atoms/molecules [12]. Cluster injection is similar to ionisation injection except it is the space charge force of the ions in a cluster which holds electrons close to the core. Thus, the cluster acts as a source of charge which can be subsequently liberated and trapped in the plasma wave.

Experimental setup

The experiment was performed in the Gemini Target Area 3 using an $f/40$ focusing geometry. This facility provides 10 J of energy in a 45 fs pulse in an average spot measured using the lower power focal spot mode of ($35\times50\pm3$ µm). The low power focal spot data combined with on-shot estimates of laser energy obtained from a leakage of the full power laser and the pulse duration using a frequency-resolved optical gating diagnostic [13] provides an estimate of the normalised vector potential of the interaction $a_0 = 1.38 \pm 0.15$.

The target was a 10 mm gas jet with an inner diameter of 1mm and a length from orifice to the exit of 7.6 mm. Three different gases were pulsed through this gas jet, helium (self-injection), helium+1% nitrogen (ionisation injection) and methane (cluster injection). These gases inject electrons in different ways into the plasma wave and will result in varying properties for the generated electron beam and betatron radiation. The electrons were dispersed using a dipole magnet onto a scintillating LANEX screen [14] which is imaged using a cam-

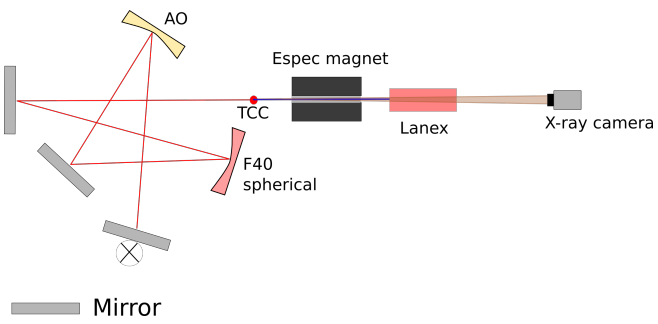

Figure 1: Experimental arrangement for study of laser wakefield acceleration in gas jet targets.

era, this diagnostic is collectively referred to as the electron spectrometer. The position of the scintillation light along the LANEX screen provides the energy of the electron beam and the intensity of the scintillation light can be used to infer the charge of the electron beam. The radiation was measured using an indirect detection x-ray camera Andor iKon-L located 157 ± 1 cm from the interaction point. The detector has a caesium iodide scintillation layer which converts the x-rays into visible light with a certain quantum efficiency [15]. The x-rays travel through a filter pack which consists of sample materials of varying atomic number and thickness. By calculating the expected transmission for a synchrotron source, we can determine the critical energy of the incident beam and the flux of photons for each shot [16]. The probe beam was used to diagnose the conditions of the plasma during the interaction by performing interferometry. In Figure 2 we can see the interferometry of the laser channel formed with helium and methane in a gas jet. We can see that the methane plasma channel is slightly longer. This is due to energy deposition being substantially larger in a clustered medium. We time the probe beam to arrive when the main laser pulse exits the medium, which for such long targets is ≈ 40 ps. This gives the plasma channel time to expand by the time that the interaction was probed.

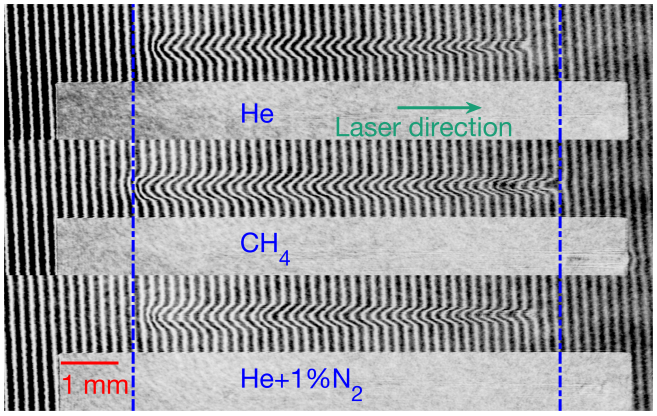

Figure 2: Interferometric data from helium (top) and methane (bottom) data sets. The laser pulse is incident from the left hand side.

Results

The density for each target was chosen such as to maximise the charge observed on the electron spectrometer. The densities for the various datasets of helium, helium+1% nitrogen and methane are 2.3 ± 0.1, 1.7 ± 2 and 3.2 ± 0.2 $\times 10^{18}$cm^{-3} respectively. There are notable differences in the energy spectrum for the various targets. On individual shots, the self-injected case, in Figure 3 consists of small peaks. The ionisation/cluster injection cases in Figure 4 and 5 do not show mono-

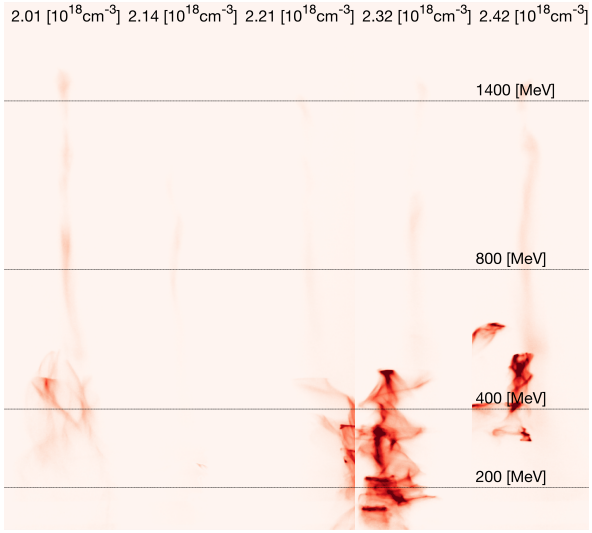

Figure 3: Electron spectra generated by self-injection in He gas. The plasma density increases from left to right.

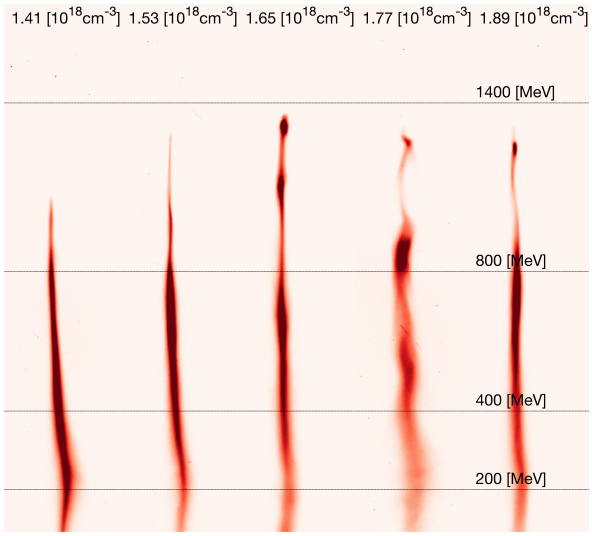

Figure 4: Electron spectra generated by ionisation injection in mixed gas (99% He, 1% N_2). The plasma density increases from left to right.

energetic peaks but broad energy spread electron beams. The charge for these beams is significantly higher than the self-injected case. We can plot the flux of the betatron radiation for each of these different media, which shows that ionisation injection is the source with the highest flux of photons.

Discussion

In the helium dataset, electrons are injected into the accelerator through the wave-breaking of the plasma wave, also known as self-injection. As wave-breaking is sensitive to modulations in plasma density along the accelerator length and imperfections in the quality of the

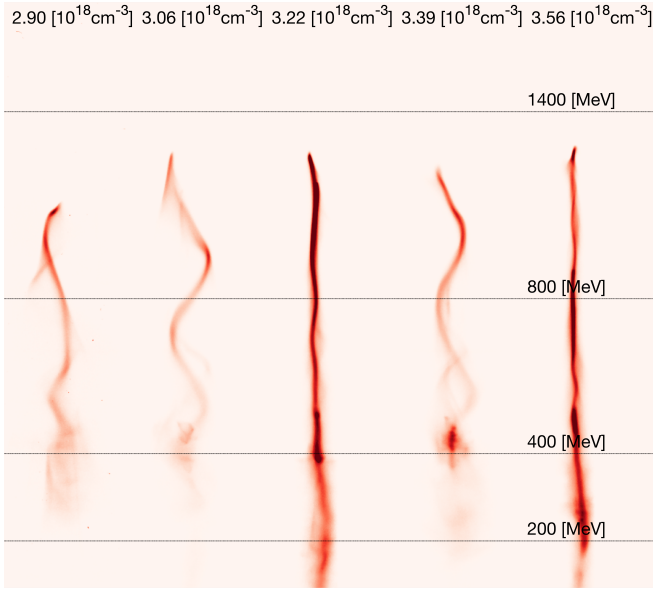

Figure 5: Electron spectra generated by cluster injection in methane gas. The plasma density increases from left to right.

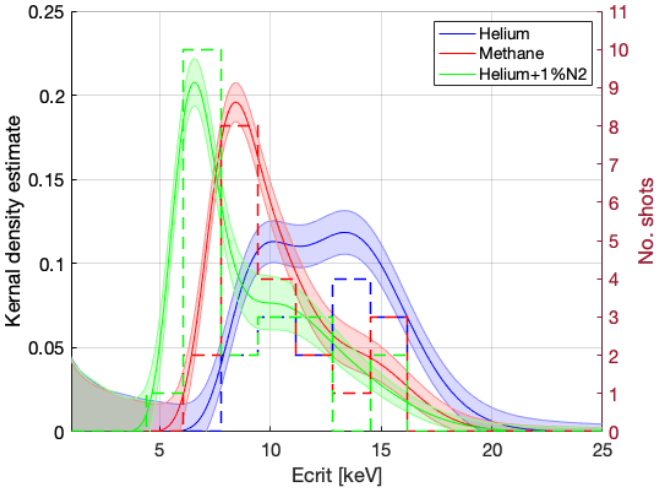

Figure 6: Histogram (right) and Kernel density estimate (left) of the critical x-ray energy observed across the various datasets.

high-power laser focus [17]. Thus, though the electrons from self-injection do reach higher maximum energies than the ionisation/cluster injection cases, the energy spectrum is inconsistent shot-to-shot. This deviation in electron beam energy can be seen to impact the critical energy of the betatron radiation generated by this source in Figure 6. The betatron radiation generated in the self-injection case reaches a mean critical energy of 14.1 ± 4.0 keV. This is higher than the mean critical energy for cluster injection of 8.4 ± 1.4 keV or the ionisation injection case of 6.7 ± 0.9 keV as seen in Figure 6. This can be explained by the higher electron beam energies from self-injection. This is enhanced by the fact

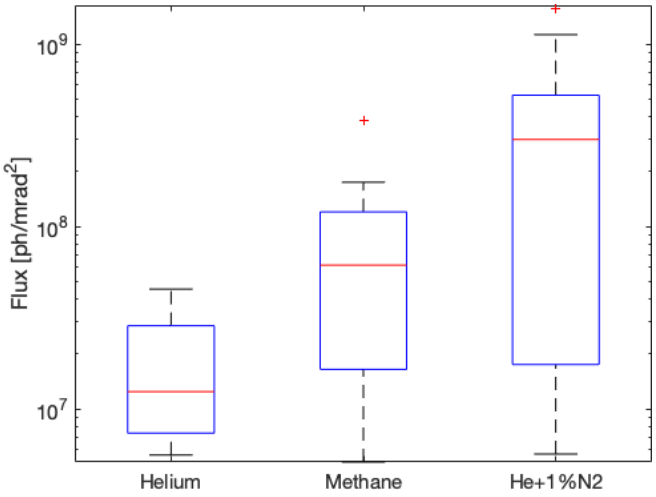

Figure 7: Box and whisker plot showing the flux estimates across the various datasets. Black line is the min/max of the data set, red line represents the median of the data set and the blue box is the interquartile range.

that the electrons in the wave-breaking case are oscillating with a larger oscillation radius. We see, though, that the enhanced stability of the ionisation/cluster injection is visible in the stability of the critical energy of the betatron beam.

The cluster injection electron spectra exhibit significantly higher transverse momentum than the other two cases, as is evident by the oscillations in the non-dispersion direction for the electron spectrometer images in Figure 5. This does not appear to increase the critical energies significantly, when compared to the ionisation injection case. One explanation for this is that, as the laser pulse is being depleted, the hosing instability [18] causes the entire accelerating cavity to oscillate. This imparts momentum onto the electron beam depending on their position in the accelerating cavity. The presence of these large oscillations also coincides with the reduction of charge below 400 MeV. This supports the hosing hypothesis as the increase in transverse momentum would increases the divergence of the beam and for particles with less around 400 MeV, the divergence is large enough for the particles to be ejected from the accelerator. The increased rate of laser pulse depletion could arise from the presence of clusters in the medium which are known to enhanced the absorption of laser energy into the medium[19]. The flux of the x-rays in the ionisation/cluster injection case is also significantly greater than the self-injection case. This is attributed to the increased electron beam charge in the ionisation/cluster injection case as is seen in Figure 3,4 and 5.

Conclusion

We have shown that the injection mechanism for electrons in a wakefield accelerator influences the properties of the betatron radiation. Self-injection in a gas jet generate betatron radiation with higher critical energies. Ionisation and cluster injection generate radiation of a higher flux than self-injection. The critical energies for ionisation and cluster injected electron beams also exhibits a lower spread than for self-injection.

1 Acknowledgements

We acknowledge STFC grants: ST/J00262/1 and ST/P000835/1 for funding the John Adams Institute for Accelerator Science.

References

[1] T. Tajima and J. M. Dawson. Laser electron accelerator. *Physical Review Letters*, 1979.

[2] S P D Mangles, C D Murphy, Z Najmudin, et al. Monoenergetic beams of relativistic electrons from intense laser-plasma interactions. *Nature*, 2004.

[3] J. Faure, Y. Glinec, A. Pukhov, et al. A laser plasma accelerator producing monoenergetic electron beams. *Nature*, (September), 2004.

[4] C G R Geddes, C S Toth, J Van Tilborg, et al. A laser plasma accelerator producing monoenergetic electron beams. *Nature*, 431, 2004.

[5] Antoine Rousse, Kim Ta Phuoc, Rahul Shah, Alexander Pukhov, Eric Lefebvre, Victor Malka, Sergey Kiselev, Fréderic Burgy, Jean-Philippe Rousseau, Donald Umstadter, and Daniéle Hulin. Production of a kev x-ray beam from synchrotron radiation in relativistic laser-plasma interaction. *Physical Review Letters*, Sep.

[6] S Kneip, C McGuffey, J L Martins, S F Martins, C Bellei, V Chvykov, F Dollar, R Fonseca, C Huntington, G Kalintchenko, A Maksimchuk, S P D Mangles, T Matsuoka, S R Nagel, C A J Palmer, J Schreiber, K Ta Phuoc, A G R Thomas, V Yanovsky, L O Silva, K Krushelnick, and Z Najmudin. Bright spatially coherent synchrotron X-rays from a table-top source. *Nature Physics*, 6:980, Oct 2010.

[7] J M Cole, J C Wood, N C Lopes, et al. Laser-wakefield accelerators as hard x-ray sources for 3D medical imaging of human bone. *Scientific reports*, 5:13244, 2015.

[8] A Modena, Z Najmudin, A E Dangor, C E Clayton, K A Marsh, C Joshi, V Malka, C B Darrow, C Danson, D Neely, and F N Walsh. Electron acceleration from the breaking of relativistic plasma waves. *Nature*, October 1995.

[9] A. Pak, K. A. Marsh, S. F. Martins, W. Lu, W. B. Mori, and C. Joshi. Injection and trapping of tunnel-ionized electrons into laser-produced wakes. *Physical Review Letters*, January 2010.

[10] C. E. Clayton, J. E. Ralph, F. Albert, et al. Self-guided laser wakefield acceleration beyond 1 GeV using ionization-induced injection. *Physical Review Letters*, 2010.

[11] M. Chen, E. Esarey, C. B. Schroeder, C. G R Geddes, and W. P. Leemans. Theory of ionization-induced trapping in laser-plasma accelerators. *Physics of Plasmas*, 2012.

[12] O. F. Hagena. Cluster Formation in Expanding Supersonic Jets: Effect of Pressure, Temperature, Nozzle Size, and Test Gas. *The Journal of Chemical Physics*, 56(5):1793, 1972.

[13] Daniel J. Kane and Rick Trebino. Single-shot measurement of the intensity and phase of an arbitrary ultrashort pulse by using frequency-resolved optical gating. *Opt. Lett.*, May 1993.

[14] A. Buck, K. Zeil, A. Popp, et al. Absolute charge calibration of scintillating screens for relativistic electron detection. *Review of Scientific Instruments*, 2010.

[15] J.C.Wood. Calibration of the clf andor ikon indirect detection camera. *CLF Annual report*, 2017.

[16] J.C.Wood. Enhanced betatron radiation from a laser wakefield accelerator in a long focal length geometry. *CLF Annual report*, 2017.

[17] S. Corde, C. Thaury, A. Lifschitz, G. Lambert, K. Ta Phuoc, X. Davoine, R. Lehe, D. Douillet, A. Rousse, and V. Malka. Observation of longitudinal and transverse self-injections in laser-plasma accelerators. *Nature Communications*, 4, 2013.

[18] CF Dong, TZ Zhao, K Behm, PG Cummings, J Nees, A Maksimchuk, V Yanovsky, K Krushelnick, and AGR Thomas. High flux femtosecond x-ray emission from the electron-hose instability in laser wakefield accelerators. *Physical Review Accelerators and Beams*, 2018.

[19] T. Ditmire, T. Donnelly, A. M. Rubenchik, R. W. Falcone, and M. D. Perry. Interaction of intense laser pulses with atomic clusters. *Phys. Rev. A*, May 1996.